Journal of Chromatography B, 912 (2013) 65–74

Contents lists available at SciVerse ScienceDirect

Journal of Chromatography B

journal homepage: www.elsevier.com/locate/chromb

Electrochemically grown imprinted polybenzidine nanofilm on multiwalled carbon nanotubes anchored pencil graphite fibers for enantioselective micro-solid phase extraction coupled with ultratrace sensing of D- and L-methionine

Bhim Bali Prasad*, Amrita Srivastava, Indu Pandey, Mahavir Prasad Tiwari

Analytical Division, Department of Chemistry, Faculty of Science, Banaras Hindu University, Varanasi 221005, India

ARTICLE INFO

Article history:
Received 10 August 2012
Accepted 3 October 2012
Available online 11 October 2012

Keywords:
Electropolymerization
D- and L-methionine
Molecularly imprinted micro-solid phase extraction pencil graphite fiber
Enantioseparation
Differential pulse cathodic stripping voltammetry

ABSTRACT

An alternative method is presented for the modification of pencil graphite fibers using surface imprinting technology. In this new approach, we have adopted surface initiated electropolymerization of benzidine monomer, with simultaneous imprinting of template (D- and L-methionine), on carboxylated multiwalled carbon nanotubes anchored pencil graphite fiber. This yielded a nanostructured ultrathin imprinted film (58.3 nm) uniformly coated all along the perimeter and length of pencil graphite fiber, for micro-solid phase extraction with substantial adsorption capability. The same film is coated over the exposed tip of the pencil graphite fiber to serve as a complementary molecularly imprinted polymer-sensor. Both extraction and sensing devices are not capable to measure the stringent limit (0.016 ng mL^{-1}) of clinical detection of methylenetetrahydrofolate reductase (MTHFR) gene mutation caused by acute methionine depletion, when used alone. However, on combination of both techniques, a successful enantioselective analysis of D- and L-methionine with excellent analytical figures of merit [limit of quantitation range: 0.03–30.00 ng mL^{-1}, limit of detection: 0.0098 ng mL^{-1} (RSD = 2.04, $S/N = 3$)] could be achieved without any problem of non-specific false-positive contribution and cross-reactivity, in real samples.

1. Introduction

Amino-acid enantiomers have different physiological activities depending on their absolute configurations. L-Amino acids are main structural components of proteins and enzymes. Their isolation from racemic mixtures with low-cost, high-efficiency, and large-scale production is apparently tedious and challenging task. On the other hand, D-amino acids do not participate in protein synthesis, except generating toxicity in functioning of living organisms.

Recently, the chemical separation of racemic mixtures of amino acids has been made employing several non-chromatographic (viz., preferential crystallization, enzymatic kinetic resolution, chemical resolution, and membrane) and chromatographic (viz., gas chromatography, high-performance liquid chromatography (HPLC), capillary electrophoresis, and chiral-ligand exchange chromatography) methods with the use of suitable chiral selectors [1,2]. However, both methods were of narrow scope owing to their limitations against large-scale separation with high-throughput screening, low-cost, high efficiency, and simplicity in terms of instrumentation, methodology, labor and time. Micro-solid phase extraction (MSPE) has been most attractive sample preparation method with several advantages over time and solvent consuming conventional processes like liquid–liquid extraction and solid-phase extraction. Nowadays, MSPE is considered to be better than liquid-phase microextraction (LPME) and solid-phase microextraction (SPME), in terms of the ease of operation, time saving, and moreover, the minimal need of organic solvent to obviate harmful effect both on the environment and operators.

Insofar as SPME is concerned, analytes are not extracted quantitatively from the sample matrix. However, the MSPE technique has not only the advantages of SPME, but can also be used for the higher enrichment factor and exhaustive recovery. This is because of the larger volume of MSPE phase (sample volume to solid phase matrix ratio $\geq 10^4$) as compared to SPME, under the same extraction conditions [3]. In this context, a novel approach of molecularly imprinted micro-solid phase extraction (MIMSPE) has revolutionized the separation field by achieving high level of selectivity in complicated matrix of real samples, with the advent of molecularly imprinted polymer (MIP) technology [4–7]. MIPs are customized synthetic polymers with specific molecular

* Corresponding author. Tel.: +91 9451954449; fax: +91 54222368127.
E-mail address: prof.bbpd@yahoo.com (B.B. Prasad).

1570-0232/$ – see front matter © 2012 Elsevier B.V. All rights reserved.
http://dx.doi.org/10.1016/j.jchromb.2012.10.010

recognition ability, and within them a great deal of specific cavities designed for a target molecule (viz., the template molecule) is distributed. These cavities are complementary to the target molecule in shape, size, and functional groups. However, the use of MIPs as chiral selectors is still far from the property of solid extractors owing to their poor performances as a result of the low mass transfer kinetics involved. Recently, chiral cavities specific for one of the glutamic acid enantiomers with high binding kinetics, following surface-imprinting approach, has successfully been designed [1]. In the past few years, intrinsic conducting polymers with conjugated double bonds have attracted much attention because of their multifunctional properties and potential applications as ion exchangers, catalysts, chemical sensors and materials for separation. Especially, electrochemically synthesized polypyrrole has extensively been used owing to emphasized synthesis and higher conductivity over many other conducting polymers [8]. Electrochemical method is apparently advantageous to prepare such materials for modifying solid sensors or SPME fibers in many respects such as porous structure, inexpensive and easy preparation, long life time, strong interaction, high thermal stability, reproducible preparation, and strong adhesion of coating to the metal wire or other fiber supports [8]. Furthermore, the thickness of coating could be controlled by implicating optimized electrochemical conditions. Despite the extensive development of MIP sensors adopting electrochemical approach [9], it is rather surprising that the electrochemically modulated SPME/MSPE devices have seldom been studied incorporating molecular imprinting matrices [10]. This could be due to the insulating character of traditional MIP (acrylic or vinylic based) systems. In our earlier work [4–6], we have precluded the novel approach of electrochemical fabrication of MIMSPE fibers. Therefore, we have resorted, for the first time, to develop an electrochemically synthesized MIP (EC-MIP) for methionine (met) isomers in polybenzidine (PBz) texture, invoking surface imprinting technology on the surface of functionalized multiwalled carbon nanotubes (MWCNTs-COOH) anchored pencil graphite fibers. The application of functionalized MWCNTs is quint essential to produce a nanostructured film with high surface area, conductivity, tensile strength, and chemical stability to offer a strong accumulation surface for MSPE and stripping voltammetry. Such electrochemically grown MWCNT-conducting PBz film can be used as MIMSPE fiber for straightforward adsorption and desorption involving small volumes. It should be noted that MIMSPE under electrochemically controlled operation was not feasible in this work. This was mainly due to the obvious difficulty in dipping electrodes while performing extraction and desorption in small volume of liquid. Therefore, we have decided to adopt a combination approach of the straightforward MIMSPE [for the selective adsorption of target analyte (met isomers)] and complementary EC-MIP sensor [for their electrochemical ultratrace detection] so as to attain simultaneously the dual preconcentrations and hence high sensitivity of the measurement. The pre-treatment (deproteinization, ultrafilteration, centrifugation, etc.) of biological fluids in ultratrace analysis was avoided because this might lead inaccuracies in the final results. Instead, the dilution is recommended by several folds so as to mitigate the matrix effect to a large extent and also to move the analysis in the ultratrace ranges. It is to be noted that neither MIMSPE nor complementary EC-MIP sensor can analyze the ultratrace amount of the analyte, when used alone. Thus, the hyphenation of both techniques is inevitable in this work.

L-Met is an essential amino acid found in proteins, foods, and pharmaceuticals. Any small deficiency as compared to control level ($1.49–5.96\ \mu g\ mL^{-1}$) might manifest AIDS and HIV infection, toxemia, muscle paralysis, and depression [11,12]. Its supplementation is the treatment of AIDS associated mylopathey [13] as well as cancer [14]. On the contrary, met-depletion is reportedly necessary in some cases to inhibit the tumor growth in preclinical model. The met depletion could be achieved by the use of methioninase (an antitumor agent). The prescribed met depleted level, preferably best to be less than $14.92\ ng\ mL^{-1}$, was detected using conventional met detection methods [15]. However, ultratrace level of met ($0.016\ ng\ mL^{-1}$ after 250 times dilution) in plasma manifests 677 C→T mutation in one or both alleles of the MTHFR gene caused by an acute met depletion [16]. Literature survey revealed that the determination of met had been feasible mainly by HPLC [16–20], capillary electrophoresis [21], and flow-injection bio-amperometric method [22]. Most of these methods, however, involved a costly set-up with time consuming complex extraction processes, and were inefficient to yield quantitative (100%) results. There were also few reports on the application of electroanalytical methods for the determination of met [22–25]. However, none of the aforesaid methods are capable to achieve very stringent limit ($\leq 0.016\ ng\ mL^{-1}$) of detection of met in dilute real samples. This work demonstrates the role of proposed combination (MIMSPE/MIP sensor) in enantioselective analysis of D- and L-met isomers, without any cross-reactivity and false-positives, by means of twice successive preconcentrations during simultaneous extraction and sensing experiments.

2. Experimental

2.1. Chemicals and reagents

Benzidine (Bz), MWCNTs (internal diameter 2–6 nm, outer diameter 10–15 nm, length 0.1–10 μm, and purity > 90%), D- and L-met and all interferents were purchased from Aldrich (Steinheim, Germany). Solvents, dimethylformamide (DMF), acetic acid (AcOH) and aq. ammonia (about 25% NH_3) were procured from Spectrochem Pvt. Ltd. (Mumbai, India). Standard stock solutions of D- and L-met ($1.00\ \mu g\ mL^{-1}$) were prepared using deionized triple-distilled water (conducting range $0.06–0.07 \times 10^{-6}\ S\ cm^{-1}$). All working solutions of D- and L-met were prepared daily by an appropriate dilution with triple distilled water. The pharmaceutical sample analyzed was an amino-acid capsule (ALAMIN-M-FORTE, Albert David Ltd., Ghaziabad, India). The capsule was dissolved in water, filtered, and diluted to the desired level of analyte concentration. Human blood plasma samples were procured from a local pathology lab and stored in a refrigerator at ~4 °C, before use. Pencil leads (2B grade) were purchased from Hi Par, Camlin Ltd. (Mumbai, India).

2.2. Equipments

MIMSPE pencil graphite fiber (1.5 cm exposed length) was used for the preconcentration of template. Extracts, desorbed from this fiber, were analyzed using a voltammetric analyzer/stripping voltammeter [Model 264 EG and G Princeton Applied Research (PAR), USA] in conjunction with an electrode assembly X–Y recorder (PAR Model RE 0089) following differential pulse cathodic stripping voltammetric (DPCSV) technique. In the three electrode system, a pencil graphite electrode ($1.96 \times 10^{-3}\ cm^2$) [duly modified with the same coating materials as used for MIMSPE pencil graphite fiber, henceforthwith referred as EC-MIP sensor], a standard Ag/AgCl electrode with porous vicor frit, and a platinum electrode were used as working, reference and auxiliary electrode, respectively. Electropolymerization was performed on an electrochemical analyzer [CH instruments, USA, model 1200 A]. FT-IR characterizations of materials, scrapped from the modified pencil leads in KBr pellets as disc, were performed with Varian 3100 FT-IR (USA). Morphological images of MIP-modified pencil graphite fibers were recorded on a scanning electron microscope

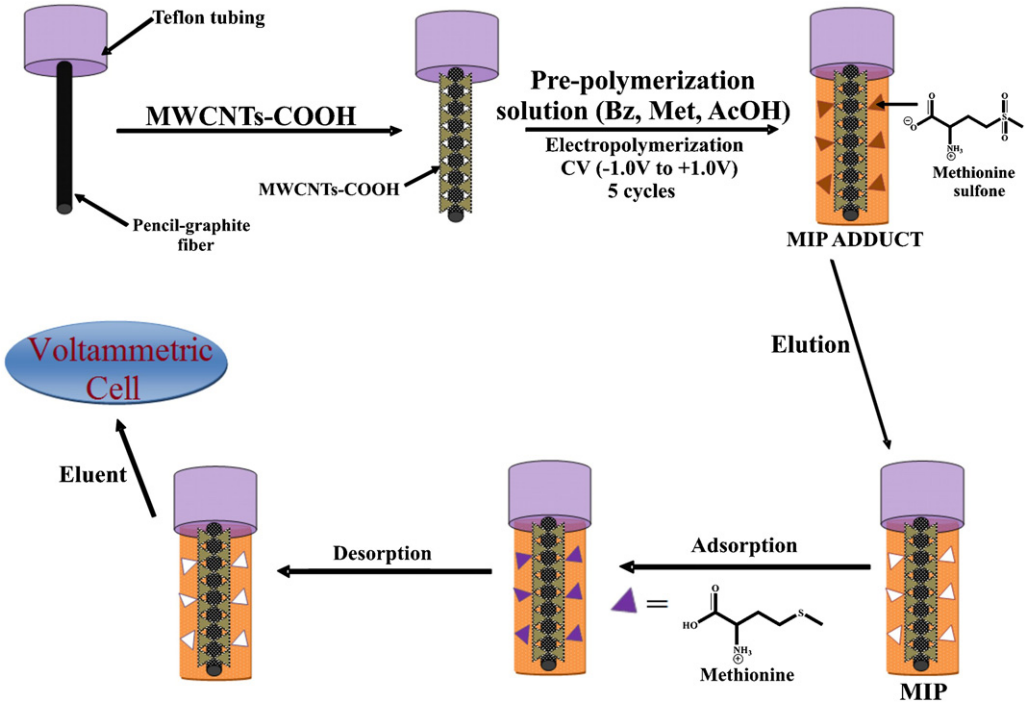

Scheme 1. Fabrication of MIMSPE fiber for methionine.

(SEM) [JEOL, JSM, Netherlands, Model 840 A]. All experiments were carried out at 25 ± 1 °C.

2.3. MIMSPE pencil graphite fiber preparation

2.3.1. Acid treatment of MWCNTs

MWCNTs-COOH was prepared following a known recipe [26] by the reaction between MWCNTs (0.50 g) and concentrated nitric acid solution (60 mL) at 100 °C for 12 h.

2.3.2. Grafting of MWCNTs-COOH onto the pencil graphite fiber surface

Pencil graphite fiber, 5.0 cm in length and 0.5 mm in diameter, was first pretreated with 6 M HNO_3 for 15 min and then washed with water to activate its surface. Subsequently, the surface was smoothened by rubbing with soft cotton. This fiber was inserted into a Teflon tube where 1.5 cm length of pencil graphite lead was exposed out at one end and electrical contact was made by soldering a copper wire through other end. An aliquot of MWCNTs-COOH (suspension in DMF, 20 mg mL^{-1}) was pre-coated on the activated fiber surface.

2.3.3. Development of EC-MIP film

EC-MIP film coated MIMSPE fibers were obtained by immersing MWCNTs-COOH modified pencil graphite fibers into the pre-polymerization solution (containing 0.05 mM D- or L-met, 0.1 mM benzidine, and 0.1 M AcOH) followed by electropolymerization under five consecutive cyclic voltammetric (CV) scans, in the potential range of −1.0 V to +1.0 V, at an optimized scan rate of 125 mV s^{-1}. After the electropolymerization, the complete retrieval of template from the MIP-template adduct was ensured by soaking MIMSPE fibers into aq. ammonia under dynamic mechanical stirring until no current response of template was noticed by DPCSV. The non-imprinted polymer (NIP)-immobilized MWCNTs-COOH coated pencil graphite fibers were also prepared, but without adding the template in the pre-polymerization mixture. Although the complementary EC-MIP modified pencil graphite electrode was used as an MIP-sensor for met detection, its modification mode is somewhat different than that for MIMSPE fiber. Whereas MIMSPE fiber was used as an extraction fiber duly modified all along the cylindrical surface of graphite fiber, the EC-MIP sensor was made subjecting only three consecutive CV cycles, for developing a nanofilm architecture of imprinted PBz, over the tip of the electrode.

2.3.4. MIMSPE-DPCSV procedure

MIMSPE was performed by a direct immersion method, without implicating any electrochemically controlled extraction. Herein, the homemade MIMSPE device, i.e. the modified pencil graphite fiber (1.5 cm in length) fixed to a Teflon tube was dipped in 10.0 mL test sample (taken in a small cylindrical glass vial of 20.0 mL capacity, sample pH adjusted to 2.0 after requistic dilution). The stirring was made with a magnetic stirring bar (size 7.0 mm × 2.0 mm) at 600 rpm for 20 min maintaining speed just enough to a vortex formation in the solution. Non-specific adsorption from test samples was curtailed simply by multiple washing (n = 2, 0.4 mL) with water. After washing with water, MIMSPE graphite fiber was subjected to analyte desorption in a solvent (0.4 mL aq. ammonia) taken in a small plastic tube (0.5 mL capacity), under magnetic stirring (for this purpose, a small stirring bar, 2 mm × 0.4 mm, was introduced in the desorption chamber). Extracted amount was determined by DPCSV measurement of the entire solution of the desorbed analyte after dilution to 10.4 mL with phosphate buffer solution and final adjustment of overall pH to 2.0 (with few drops of 0.1 M HCl) in a voltammetric cell. The other optimized operating conditions for DPCSV measurement with EC-MIP sensor were: analyte accumulation potential, +0.6 V respective to Ag/AgCl; analyte accumulation time, 60 s; supporting electrolyte, phosphate buffer solution (pH = 2.0); scan rate, 10 mV s^{-1}; pulse amplitude, 25 mV; pulse width, 50 ms. At such operating conditions, the maximum development of DPCSV current for analyte was realized presumably because of the generation of reactive oxygen species as charge transfer mediators, consequent upon the preanodization of the electrode at +0.6 V for 60 s duration. All DPCSV runs for each

Table 1
Comparison between analytical results of L-met obtained with different combination approaches in aqueous samples.

Hyphenated system	[Analyte]$_{taken}$ (ng mL^{-1})	Sample volume (mL)	Volume eluted (mL)	[Analyte]$^{a}_{desorbed}$ (ng mL^{-1})	EF[b]	Recovery[c] (%)	RSD (%) (n = 3)
MIMSPE based on MWCNTs-COOH anchored imprinted PBz-modified pencil graphite fiber involving DPCSV detection with bare pencil graphite electrode	0.50	10	0.4	–	–	–	–
	0.75	10	0.4	–	–	–	–
	1.00	10	0.4	7.75 ± 0.08	7.75	31.88	1.08
MIMSPE based on MWCNTs-COOH anchored imprinted PBz-modified pencil graphite fiber involving DPCSV detection with pencil graphite electrode modified only with MWCNTs-COOH	0.50	10	0.4	–	–	–	–
	0.75	10	0.4	–	–	–	–
	1.00	10	0.4	8.26 ± 0.04	8.26	33.06	0.55
MIMSPE based on MWCNTs-COOH anchored imprinted PBz-modified pencil graphite fiber involving DPCSV detection with pencil graphite electrode modified only with MIP	0.50	10	0.4	–	–	–	–
	0.75	10	0.4	–	–	–	–
	1.00	10	0.4	8.85 ± 0.27	8.85	35.42	2.99
MIMSPE based on pencil graphite fiber (without MWCNTs) involving DPCSV detection with complementary EC-MIP sensor	0.50	10	0.4	–	–	–	–
	0.75	10	0.4	–	–	–	–
	1.00	10	0.4	4.97 ± 0.14	4.97	19.86	2.72
MIMSPE based on MWCNTs (pure)-anchored imprinted PBz-modified pencil graphite fiber involving DPCSV detection with pencil graphite electrode modified with complementary MWCNTs/EC-MIP sensor	0.50	10	0.4	–	–	–	–
	0.75	10	0.4	10.87 ± 0.32	14.50	57.99	2.92
	1.00	10	0.4	15.76 ± 0.58	15.76	63.05	3.67
MIMSPE based on MWCNTs-COOH anchored imprinted PBz-modified pencil graphite fiber involving DPCSV detection with pencil graphite electrode modified with complementary MWCNTs-COOH/EC-MIP sensor	0.50	10	0.4	12.44 ± 0.34	24.89	99.58	2.74
	0.75	10	0.4	18.86 ± 0.16	25.15	100.60	0.85
	1.00	10	0.4	25.41 ± 0.21	25.41	101.35	0.83

[a] [Analyte]$_{desorbed}$ denotes the concentration of desorbed amount (i.e. analyte amount eluted by the fiber/optimized volume of the desorbing solvents).
[b] Enrichment factor: [analyte]$_{desorbed}$/[analyte]$_{taken}$.
[c] Recovery: (amount of desorbed analyte)/(amount of analyte in sample).

concentration of test analyte were quantified using the method of standard addition. The limit of detection (LOD) was calculated as $3S_b/m$, where S_b is the standard deviation of 16 blank determinations at the peak base and m is the slope of calibration curve between DPCSV current and analyte concentration [27].

3. Results and discussion

3.1. MIMSPE pencil graphite fiber characteristics

Development of EC-MIP film on the carboxylated MWCNTs-modified pencil graphite fiber is illustrated in Scheme 1. The pencil graphite fiber is consisted of high proportion of graphite. This type of fiber was preferred because of its excellent adsorption characteristics; and moreover, it is economic and stable against any temperature variation. Before electropolymerization, the initial grafting of MWCNTs-COOH onto the surface of pencil graphite fiber facilitated a stronger anchoring of imprinted PBz film to its surface through covalent bonding and inherent π–π interactions. As a consequence, MWCNTs functionalized with —CONH groups had higher capacity to retain the test analyte than pure MWCNTs; and thus, enrichment factor was improved dramatically with functionalized MWCNTs (Table 1). Furthermore, simple imprinted PBz or MWCNTs (unmodified) interspersed imprinted PBz-modified pencil graphite fibers were found inferior to MWCNTs-COOH anchored imprinted PBz film in responding quantitative (100%) template extraction (Table 1). This could be attributed to the high adsorption ability on account of relatively large surface-to-volume ratio provided by MWCNTs-COOH (transformed in MWCNTs-CONH) in nano-structured film, electrochemically coated to either all along the surface of pencil graphite fiber for MIMSPE or over the tip of its surface for the fabrication of complementary EC-MIP sensor. The transformation of MWCNTs-COOH into MWCNTs-CONH, after reacting with Bz molecules, has primarily been found useful to involve hydrogen bonding interactions with the analyte (print) molecules, as depicted in Scheme 2. The electropolymerized MIP could be referred as if 'OMNMIPs' (One MoNomer MIPs) to cast higher template loading than that reportedly found with traditionally made MIP formulations [28]. This approach actually eliminates variables such as choice of functional monomer and crosslinker, the ratio of functional monomer/crosslinker which normally complicates the MIP design. The electrochemical growth of MWCNT-COOH/conductive polymer composites has ability to produce three-dimensional nano-structured film that combines the redox pseudo-capacitive charge storage mechanism of conducting polymer with the high surface area and conductivity of MWCNTs [29]. Such film should be used in the fabrication of MSPE cartridges. The main advantage of CNTs compared with conventional carbon is that CNTs help producing a relatively non-porous sorbent that eliminates mass-diffusion impediment facilitating fast desorption of analyte. Many factors, e.g. electropolymerization cycles, polymer composition, and scan rate, were also optimized and corresponding results are depicted in Supporting Information (Fig. S1). These factors are responsible to enhance specific extraction efficiency of chiral selectors. A series of experiments using different electropolymerization CV cycles (n = 2, 3, 5, 9, and 15) were accomplished in the potential window −1.0 V to +1.0 V. The film thickness could be controlled by the use of electropolymerization cycles. Fig. S1A shows the effect of number of CV cycles on the extraction efficiency of the analyte. After fifth electropolymerization cycle, the film thickness was optimized with maximum surface area and the further insertion of polymer was no longer feasible which consequently limited the extraction efficiency to a great extent. If somehow the thickness of adsorbent is amplified, this might endanger the stability of the film owing to an irreversible loss of molecular recognition

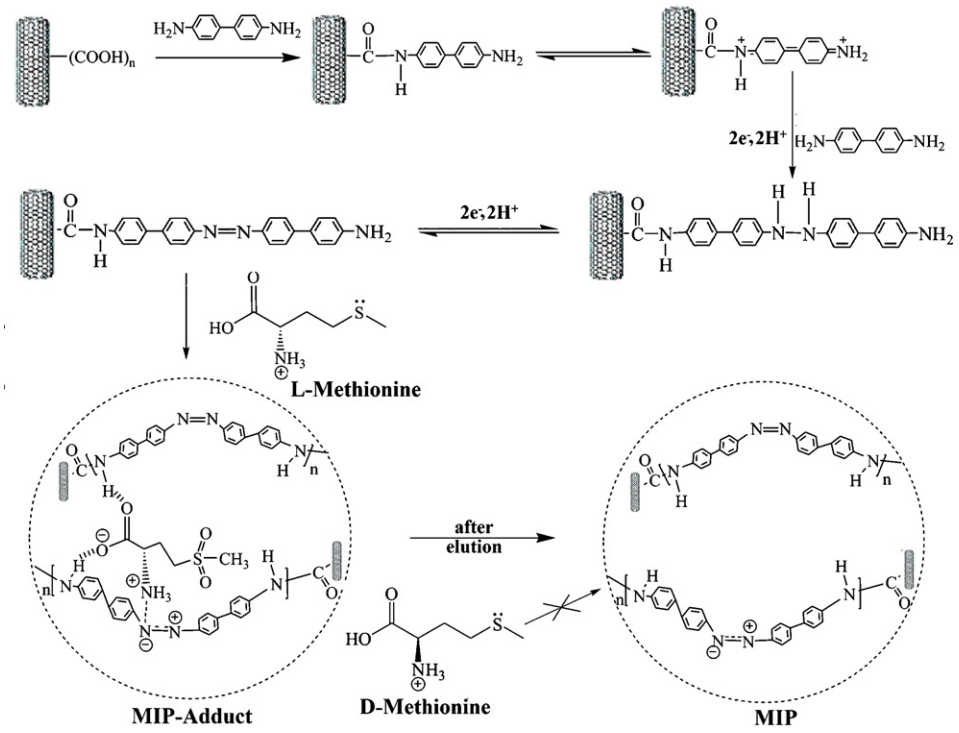

Scheme 2. Schematic illustration of enantioselective imprinting of L-met in electropolymerized MIP cavities.

sites under the stress of the successive adsorption and desorption of analyte. The other important electrochemical condition for controlling the thickness of coating layer is obviously the CV scan rate. The EC-MIP film development in this work was examined by varying CV scan rates from 100 to 200 mV s^{-1}. The optimum scan rate was found to be 125 mV s^{-1}. Applying high scan rate than this might have affected the stability of the film; and thereby, any loss of binding sites, upon adsorption–desorption cycle, resulted in a progressive loss of extraction efficiency (Fig. S1B). The optimum stoichiometry, i.e. the molar ratio between template and monomer was found to be 1:2. The higher ratio may lead to a decreasing number of binding sites owing to the paucity of template molecules requisite for generating molecular cavities in MIP network (Fig. S1C).

3.2. Morphological and spectral characterizations

Fig. S2 displays SEM images of MIMSPE fibers, in the presence and in the absence of template. Whereas the EC-MIP template adduct, apparent as coated MWCNTs flakes, on the fiber surface is non-porous (Fig. S2A), the same is appeared to be porous (Fig. S2B) upon template removal. Notably, MWCNTs anchored pencil graphite lead could not be visualized in its respective SEM image (not shown) owing to the crowed and collapsed MWCNTs, after drying. Fig. S2C reveals a uniform and homogenous coating all across the perimeter and length of pencil graphite fiber. The porosity in the EC-MIP film, after template retrieval, significantly increased the effective surface area for the adsorption of template molecules. The top-side view of the MWCNTs-COOH/MIP-modified pencil graphite fiber revealed a non-uniform coating with an average thickness of 58.3 nm (Fig. S2D).

FT-IR (KBr) spectra of template (curve A), monomer (curve B), MWCNTs-COOH/MIP-template adduct (curve C), and MWCNTs-COOH/MIP (curve D) are shown in Fig. S3. The MIP-analyte binding mechanism (Scheme 2) could be ascertained by comparing these spectra. The involvement of hydrogen bonding interaction is suggested by the downward shifting of IR bands of participating functionalities as described below:

- FT-IR (KBr) bands due to hydrophilic $-NH_3^+$ of met (3420 cm^{-1}) and azo group of imprinted PBz (1390 cm^{-1}) are shifted to 3320 and 1295 cm^{-1}, respectively (curve C), after ion-pair binding in MIP-template adduct.
- The characteristic bands of template [2950 cm^{-1} (carboxylate anion); 1710 cm^{-1}, curve A] are downwardly shifted [2760 cm^{-1} (carboxylate anion); 1650 cm^{-1} (—C=O, curve C)], consequent upon template rebinding to MIP through (—C=O···HN—) bonding.
- FT-IR (KBr) bands due to —N—H stretching (3495 cm^{-1}) and —N—H out-of-plane bending (1405 cm^{-1}) of MIP (curve D) are shifted to 3450 and 1350 cm^{-1} (curve C) suggesting an electrostatistically driven hydrogen bonding between —N—H (host) and $-COO^-$ anion (guest).
- The emergence of a typical ⟩S=O band at 1060 cm^{-1} (curve C) in MIP-template adduct suggested the print met molecules encapsulated in the imprinted cavities were instantaneously oxidized during the course of electropolymerization.

It is interesting to note that all downwardly shifted bands upon template rebinding are reinstated to their original positions upon template retrieval (curve D). Furthermore, while rebinding the template to the MIP in aqueous environment, it is the electrostatic force operating between them which strongly drive hydrogen bonding against any anticipated water-competition.

3.3. MIMSPE optimizations

Both D- and L-met enantiomers have identical characters in terms of optimizations of operating conditions. The MIMSPE fiber was immersed in the sample solution containing representative analyte (1.0 ng mL^{-1}, L-met) for 20 min and then subjected to

analyte elution using 0.4 mL of eluents, viz., ethanol, AcOH, aq. ammonia:ethanol (1:2, v/v), and aq. ammonia. Analyte recoveries were 19.89, 28.83, 44.50, and 99.23%, respectively, with these desorption solvents (Fig. S4A). Accordingly, all protic and moderate acidic solvents showed poor elutions since the electrostatic binding of template with MIP could not effectively be deactivated. On the other hand, aq. ammonia was found to be almost suitable eluent to disrupt all kind of H-bonds, without any deformation of molecular cavities, and thus quantitative (100%) recovery was obtained. Fig. S4B and C depicts dynamic desorption profiles showing that 10 min desorption time is sufficient for quantitative recovery at 30 °C, without any probability of analyte carry over inside the fiber texture.

The effect of sample volume (analyte concentration, 1.0 ng mL^{-1}) on MIMSPE efficiency was investigated. The increase in extraction (adsorption) efficiency with the sample volume up to 10 mL is due to increment in analyte uptake; the maximum uptake using 10 mL volume of sample solution may be considered to be a breakthrough volume (Fig. S4D), after that tolerance of MIMSPE fiber is gradually lost. The optimal time for MIMSPE, which responded quantitative recovery, was 20 min (Fig. S4E). Herein, the initial partitioning might have rapidly occurred with the increasing extraction time and that finally optimized to lead a limiting plateau. Furthermore, the solution pH is also considered crucial for the optimum analyte adsorption. The extraction efficiency instantly increased to yield quantitative recovery at pH 2.0, followed by sharp decline in the analyte uptake (Fig. S4F). In strong acidic medium, met exists as $-NH_3^+$ cation due to protonation which facilitates electrostatic binding. Such interactions actually help upbringing water-compatibility to the MIMSPE fiber.

3.4. Binding characteristics of imprinted polymers

To investigate the affinity of the EC-MIP, binding studies were carried out based on MIMSPE experiments. The binding isotherm of L-met to MIP was determined in the range of 1–40 ng mL^{-1}. The amount of adsorbed L-met was calculated as

$$Q = \frac{(C_0 - C)V}{m} \quad (1)$$

where Q is the amount of L-met adsorbed onto unit mass of PBz film (ng g^{-1}), C_0 and C are the concentrations of L-met in the initial solution and at the equilibrium (free template concentration) after adsorption (ng mL^{-1}), V is the volume of the aqueous phase (mL), and m is the weight (g) of adsorbent (i.e. weight of MIMSPE fiber – weight of bare pencil graphite fiber) The values of C can be calculated from the linear adsorption isotherm (Fig. 1, inset a) between $[\text{analyte}]_{\text{taken}}$ and $[\text{analyte}]_{\text{desorbed}}$ using MWCNTs-COOH/PBz modified pencil graphite fiber (Table 2; all data are not shown). Binding properties were estimated by Scatchard analysis based on the following equation [30]:

$$\frac{Q}{C} = \frac{Q_{\max}}{K_D} - \frac{Q}{K_D} \quad (2)$$

where $Q_{\max}$ represents to the apparent maximum number of binding sites and K_D is the equilibrium dissociation constant of the L-met-PBz film. With conventional MIPs prepared via non-covalent approach, Scatchard curve (Q/C vs Q) is generally represented by two secant lines that indicate the presence of heterogeneous binding sites on MIP. Interestingly, in this work, Scatchard curve (Fig. 1) is only one straight line which indicates the formation of homogeneous interaction sites in the polymeric network that led exclusively the selective adsorption of analyte molecules in MIP cavities. Herein, the predominant factor for imprinting may be considered to be a strong electrostatic force, rather than other weak hydrogen bondings, operating between one template with

Table 2
Analytical results of DPCSV measurements of L-met and D-met in an aqueous environment by combination MIMSPE/EC-MIP sensor.

Analyte	$[\text{Analyte}]_{\text{taken}}$ (ng mL^{-1})[a]	Sample volume (mL)	$[\text{Analyte}]_{\text{desorbed}}$ (ng mL^{-1})[b]	Volume eluted (mL)	EF[c]	Recovery[d] (%)	RSD[e] (%) (n = 3)	R^2[f]	t[g]
L-Met	0.03 (nd)	10.00	0.74 ± 0.02	0.4	24.71	98.85	2.5	0.99	t_{cal} = 1.81
	0.50 (nd)	10.00	12.44 ± 0.34	0.4	24.89	99.58	2.74		
	1.00 (nd)	10.00	25.73 ± 0.21	0.4	25.41	101.6 (101.6, 100.3, 100.3) {(i) 101.3, (ii): 89.24, (iii) 85.53, (iv) 40.25}	0.83		t_{tab} = 4.30
	10.00 (nd)	10.00	252.78 ± 2.50	0.4	25.28	101.1	0.98		
	20.00 (19.11)	10.00	497.60 ± 2.96	0.4	24.87	99.52	0.59		
	30.00 (29.68)	10.00	756.35 ± 11.78	0.4	24.64	98.41	1.59		
D-Met	0.03 (nd)	10.00	0.74 ± 0.01	0.4	24.88	99.55	1.68	0.99	
	0.50 (nd)	10.00	12.31 ± 0.32	0.4	24.62	98.48	2.5		
	1.00 (nd)	10.00	25.54 ± 0.50	0.4	25.54	101.1	1.96		
	10.00 (nd)	10.00	252.51 ± 2.50	0.4	25.28	101.1	0.98		
	20.00 (19.24)	10.00	509.57 ± 3.06	0.4	25.47	101.5	0.60		
	30.00 (29.52)	10.00	732.26 ± 5.80	0.4	24.69	98.78	0.78		

[a] Values in parenthesis denote met concentration determined by MIP-sensor; nd, not detectable.
[b] $[\text{Analyte}]_{\text{desorbed}}$ denotes the concentration of desorbed amount (i.e. met amount eluted by the fiber/optimized volume of the desorbing solvent).
[c] Enrichment factor: $[\text{Analyte}]_{\text{desorbed}}/[\text{Analyte}]_{\text{taken}}$.
[d] Recovery: (amount of desorbed met)/(amount of met in sample), values in parentheses indicate recoveries from three MIMSPE fibers of different batches, values in curled brackets indicate recovery after (i) 175, (ii) 180, (iii) 185, and (iv) 195 consecutive extractions by the same MIMSPE fiber regenerated on every alternate day.
[e] Relative standard deviation.
[f] R^2, Correlation coefficient.
[g] Student's t-test for comparison of results obtained by the present method (0.028, 0.48, and 0.98 ng mL^{-1}) and GC–MS method [30] (0.04, 0.74, and 1.49 ng mL^{-1}), for lower concentration level (0.03, 0.50, and 1.00 ng mL^{-1}, n = 3) of analyte, at 95% confidence level.

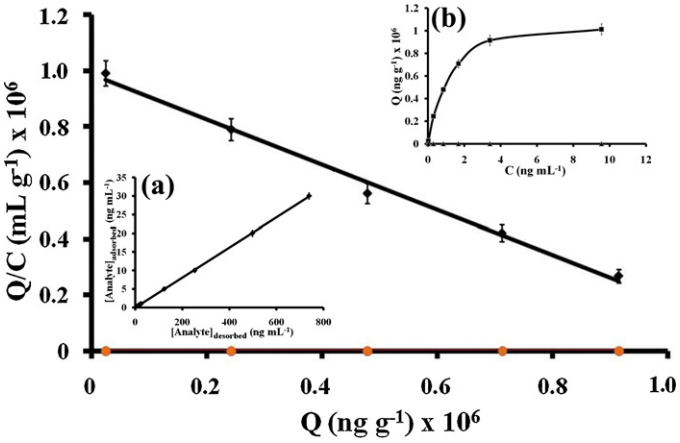

Fig. 1. Scatchard representation of the linear binding isotherm for L-met adsorption on MIMSPE (♦) and NIP-coated MSPE (●) fibers. Insets (a) shows the linear adsorption isotherm of L-met on L-met imprinted MIMSPE fiber and (b) shows the rebinding tendency of L-met (■) and D-met (▲) on L-met imprinted MIMSPE fiber.

two monomers, in spatial disposition of parallel track of two polymer chains (Scheme 2). The other plausible reason for one straight line (Fig. 1) may be attributed to the involvement of either of the adsorption types (specific or non-specific), during the course of binding experiment. In this work, any possibility of non-selective binding is ruled out, since non-specific adsorption of L-met on the NIP-coated MSPE (control) fiber was not observed (Fig. 1). Accordingly, the analyte adsorption in homogeneously imprinted binding sites on MIMSPE fiber was purely specific to lead Scatchard curve as one straight line, involving absolutely negligible non-specific contribution and false-positive, as a consequence of excellent imprinting effect. While imprinting occurred with methionine sulfone [24], an oxidized form of met under electropolymerization, normal MIMSPE was able to extract met directly from the solution on account of dominating ion-pair rebinding. The inset isotherm (Fig. 1, inset b) suggests that binding cavities are saturated revealing the maximum adsorption to the tune of 0.9×10^6 ng g^{-1}. The K_D (=1/K_a) value could be estimated from Scatchard plot as 11.80 ng mL^{-1} and the maximum number of binding sites, Q_{max}, was found to be 1.39×10^6 ng g^{-1}. The correlation coefficient (R^2) for this plot was calculated as 0.99. Furthermore, the value of free-energy change (ΔG°) for the adsorption process is calculated as −62.76 kJ mol^{-1} (since $\Delta G^\circ = -RT \ln K_a$; $K_a = 1 \times 10^{11}$ mol^{-1}). The negative ΔG° value indicates the presence of spontaneous adsorption process.

3.5. DPCSV measurements

EC-MIP sensor when used alone, responded no DPCSV current for L-met concentration 1.00 ng mL^{-1} (Fig. 2, curve a) in aqueous samples. This, however, could be found responsive by combining MIMSPE necessarily with the complementary EC-MIP-sensor (Fig. 2, curve b). To explore sensitivity of the hyphenation approach, a typical DPCSV run was recorded on EC-MIP sensor, after MIMSPE, for L-met concentration, 20 ng mL^{-1}, and applying optimized operating conditions for both the techniques. This revealed DPCSV current height to be 14-times larger than that realized by the exclusive use of EC-MIP sensor. The double preconcentration, first at the MIMSPE fiber and second at the EC-MIP sensor, enhanced the limit of detection (LOD) as much as 336-fold in aqueous samples [EC-MIP sensor: LOD = 3.36 ng mL^{-1}; MIMSPE-MIP sensor: LOD = 0.0098 ng mL^{-1}]. Analytical results for both isomers of met obtained with MIMSPE/EC-MIP sensor are summarized in

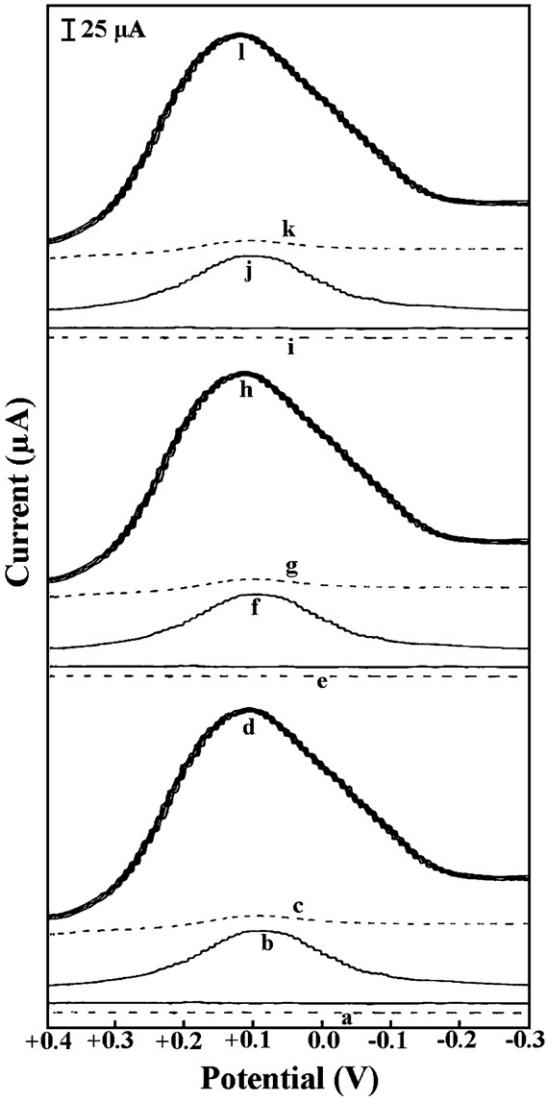

Fig. 2. DPCSV response of L-met (concentration, ng mL^{-1}): (a) 1.00 and (c) 20.00, in aqueous medium using only EC-MIP sensor; (b) 1.00 and (d) 20.00, in aqueous medium using MIMSPE/EC-MIP sensor; (e) 1.00 and (g) 20.00, in pharmaceutical sample using only EC-MIP sensor; (f) 1.00 and (h) 20.00 in human pharmaceutical sample using MIMSPE/EC-MIP sensor; (i) 1.00 and (k) 20.00, in human plasma sample using only EC-MIP sensor; (j) 1.00 and (l) 20.00, in human plasma sample using MIMSPE/EC-MIP sensor [DPCSV blank runs for different matrices are shown as base lines of (b) (aqueous sample), (f) (pharmaceutical sample), and (j) (blood plasma sample) curves].

Table 2. The associated relationship between [analyte]$_{taken}$ and [analyte]$_{desorbed}$ is an indicative of linear adsorption isotherm of met isomer(s) with their respective MIMSPE fibers. Notably, an enrichment factor of about 25-fold was achieved for both D- and L-isomers (Table 2). This reflects similar mass-transfer kinetics of both analytes in their respective MIP-coating layers, measured at identical operating conditions. Analyte recoveries for three identical samples were found to be consistently quantitative (100%) with the use of a combined MIMSPE/EC-MIP sensor device. It should be borne in mind that MIMSPE combination with gas chromatography (GC) or other conventional detection tool is not advantageous if one has to achieve stringent limits of ultra trace analysis in the real samples. Because, this cannot afford the required double preconcentration, as has been obtained in the present instance. Insofar as rigidity and reproducibility of MIMSPE fiber are concerned, any such device could be used for as many as 175 consecutive

extractions, after regeneration by the method of template removal. Subsequent decrease in recoveries was noticed when the same MIMSPE fiber, regenerated on every alternate day, was used beyond 175 extractions (Table 2). As far as precision among intra-day experiments on MIMSPE fibers of different batches is concerned, a parallel measurement for L-met (1.00 ng mL^{-1}) in aqueous environment on three MIMSPE fibers yielded quantitative recoveries with relative standard deviation (RSD) of 0.83%. This endorsed fiber-to-fiber reproducibility, and thereby the actual practicability of the proposed technique. The method ruggedness for DPCSV measurement, after MIMSPE on a single fiber regenerated after each run, was confirmed by multiple DPCSV runs of MIMSPE extracts (L-met concentration, 20.00 ng mL^{-1}; Fig. 2, curve d). Besides aqueous sample, the proposed hyphenation approach was also used for the analysis of one of the met isomers, i.e. L-met, exclusively present in human blood plasma samples. Carefully optimization of the experimental parameters has credited MIMSPE-DPCSV procedure with excellent analytical figures of merit (AFOM). Table 3 summarized the AFOM obtained, via MIMSPE/EC-MIP sensing, in the form of calibration equations for aqueous, pharmaceutical, and blood plasma samples. All linear dynamic ranges are based on the average peak-heights for at least three L-met concentrations. The average peak-heights correspond to a minimum nine DPCSV measurements made from triplicate aliquots collected from three complete experimental trials. The lowest linear concentration corresponds to the limit of quantitation, which was calculated as $10S_b/m$. The excellent R^2 demonstrates the existence of linear relationship in all cases. The LOD ($3S_b/m$) varied from 9.8 ng L^{-1} (aqueous) to 10.3 ng L^{-1} (blood plasma); the RSD values demonstrate excellent precision of LOD values at parts-per trillion concentration level (Table 3). Comparison of overall recoveries in Table 3 indicates almost no effect from the matrix composition of the unknown real samples. The almost identical slopes of the calibration curves for real samples indicate that the sample behaviors are very close to aqueous samples even after many fold dilution. The hyphenation approach was further validated by comparing results with those obtained earlier by a GC–mass spectrometry (GC–MS) [31] in the aqueous environment. The $t_{cal} < t_{tab}$ at the confidence level of 95% (Table 2) revealed although a similar order of precision in the final results obtained by both methods, the proposed method is cost-effective and highly sensitive involving rather a simple instrumentation as compared to GC–MS.

3.6. Enantioselective separation and cross-reactivity

Since the physico-chemical properties of both enantiomers are same, except for their three-dimensional orientation in space, enantioselectivity could be best measured by the virtue of imprinting effect. Notably, binding affinity of D-met was negligible (Fig. 1, inset b) when measured with L-met imprinted MIMSPE fiber, apparently because of functional constraints. The chiral imprinted sites in L-met imprinted MIP are highly matched with L-met in terms of space, structure, and spatial arrangement of action sites showing the maximum binding capacity. The reverse is true with D-met imprinted MIMSPE fiber showing chemical affinity for D-met only and excluding L-met during the course of rebinding.

Anti-interference effects on MIMSPE fibers were tested in the presence of various interferents, viz., D-met, L-cystine (L-Cys), glycine (Gly), tryptophan (Trp), ascorbic acid (AA), L-tyrosine (L-Tyr), L-histidine (L-His), L- and D-glutamic acid (L- and D-Glu), D-proline (D-Pro), cysteine (Cytn), L-phenylalanine (L-PhA), Throxine (Thr), and glutathione (GT). Accordingly, all interferents were found not to be responsive with MIMSPE device imprinted for L-met. However, with NIP-modified MSPE fiber, there were some non-specific adsorptions of D-met, Gly, L-PhA, D-Glu, and AA maximally about 40% after first water-wash (1×0.4 mL). These

Table 3
Sample behavior.

Analyte	Sample	Dilution factor	Range (ng mL^{-1})	Calibration equation	Recovery (%)	LOD (3σ; ng mL^{-1})	RSD (%) ($n = 3$)
L-Met	Aqueous sample	–	0.03–30.00	$I_p = (11.59 \pm 0.37)C + (34.98 \pm 4.30)$; $R^2 = 0.99$	98.41–101.65	0.0098	2.04
	Pharmaceutical sample	61×10^5	0.03–30.00	$I_p = (11.13 \pm 0.36)C + (32.78 \pm 4.28)$; $R^2 = 0.99$	97.94–101.58	0.0101	2.30
	Normal human blood plasma sample	5×10^4	0.03–30.00	$I_p = (11.31 \pm 0.20)C + (34.28 \pm 2.70)$; $R^2 = 0.99$	97.52–100.61	0.0099	1.10
	Human blood plasma sample of L-met deficient patient	250	6.00–30.00	$I_p = (11.27 \pm 0.47)C + (34.21 \pm 8.96)$; $R^2 = 0.99$	97.54–101.58	0.0103	2.8
D-Met	Aqueous sample	–	0.03–30.00	$I_p = (11.64 \pm 0.37)C + (32.06 \pm 4.69)$; $R^2 = 0.99$	98.48–101.58	0.0098	1.59

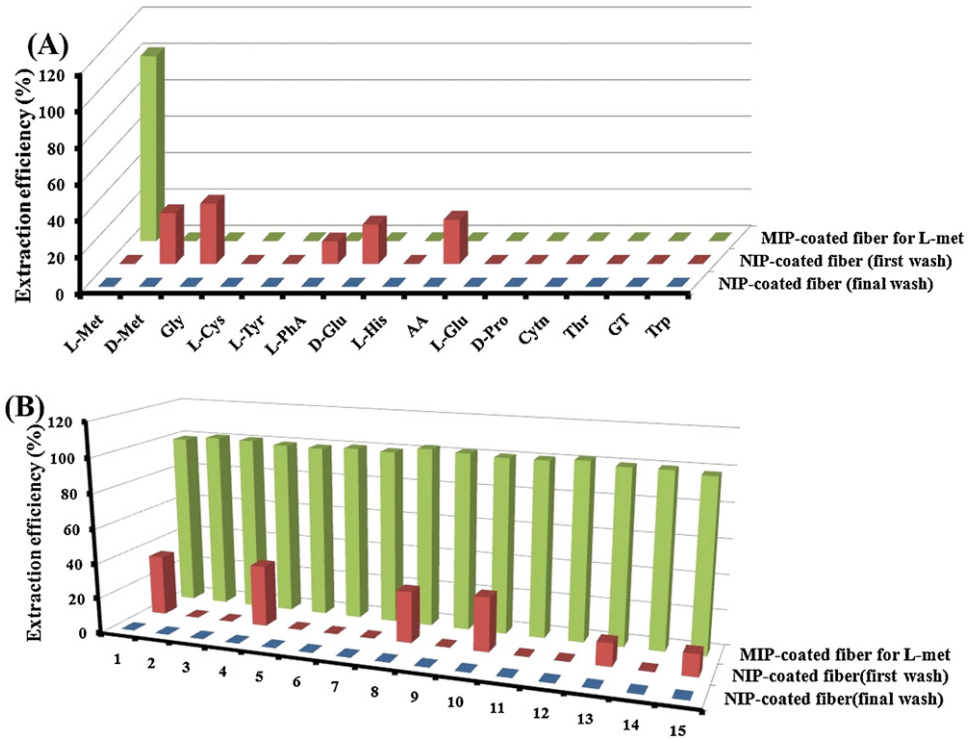

Fig. 3. (A) Extraction yields of L-met, and interferents with MIP- and NIP-coated MSPE fibers at 5.00 ng mL^{-1}; (B) extraction yields of L-met in aqueous solutions by MIP-coated and NIP-coated MSPE fibers in the presence of interferents [binary mixture of L-met (1.00 ng mL^{-1}) and interferent (10.00 ng mL^{-1})]: (1) D-Met, (2) L-Cys, (3) Gly, (4) AA, (5) L-Tyr, (6) L-His, (7) Trp, (8) D-Glu, (9) L-Glu, (10) L-PhA, (11) Cytn, (12) D-Pro, (13) Thr, (14) GT, and (15) mixture of all interferents (10.00 ng mL^{-1} each).

were, however, completely mitigated by the second water-wash (Fig. 3A). Since such non-specific adsorptions are also feasible on MIMSPE fibers, it is advisable to wash them thoroughly using 2× 0.4 mL water, when the extraction is over. Insofar as investigation related to binary mixture (template-interferent, clinical concentration ratio 1:10) are concerned in aqueous samples, a highly selective and quantitative analysis of L-met was feasible in the presence of concomitant interferents or mixture of interferents, without any cross-reactivity and false-positives (Fig. 3B). The anti-interference ability was also examined in the complicated matrix of real samples, which showed no interference and cross-reactivity; and thus quantitative recoveries for L-met were obtained (Table 3).

3.7. Application to real samples

Once the proposed method was established for aqueous solutions of test analyte, the MIMSPE fibers were subjected to analytical validation, in complex matrices of real samples. For this, human plasma samples of L-met deficient patients had to be diluted by a factor of minimum 250 for the evaluation of L-met. Such dilution actually helped to mitigate non-specific sorption due to complex matrices and a better DPCSV response was achieved with quantitative recovery (Table 3). Any dilution less than 250-fold revealed an apparent loss in recovery presumably due to fiber fouling (Fig. S1D). Moreover, the 250-fold dilution was also necessary to move the detection in the concentration range required to diagnose MTHFR gene mutation. The normal human blood plasma containing sufficient amount of L-met had to be diluted to the extent of 5×10^4-fold in order to move the detection to ultratrace level. The pharmaceutical sample [Alamine-M-Forte] was also analyzed after dissolving in water followed by filtration and requistic dilution to ng mL^{-1} level of analyte concentration. The proposed method was found to be rugged and reproducible as evinced by the multiple DPCSV runs of MIMSPE extracts from real samples (Fig. 2, curves h, l).

4. Conclusions

MIMSPE is still in infancy, and further studies are certainly needed to fully understand the adsorption of met isomers onto nanostructured film and to ensure quantification feasible with μL volume of the sample. Although, in the present work, sample volumes used were 10 mL for each MIMSPE experiments, the most striking feature was a very small volume of eluent (400 μL) required for complete desorption of test analyte from molecular cavities of imprinted polymer network. This enhanced the enrichment factor as much as approximately 25-fold for all types of sample. This work shows, for the first time, the application of an enantioselective EC-MIP, duly immobilized on MWCNTs-COOH/pencil graphite fiber, which acts both as MIMSPE fiber and complementary EC-MIP sensor. Whereas MIMSPE has shown enantioselective quantitative extraction of D- and L-met from test samples completely free of co-extractives, its direct coupling to complementary EC-MIP sensor enabled us to analyze stringent limit of D- and L-met, without any problem of surface fouling. The method was also validated for the ultratrace analysis of L-met exclusively found in human blood plasma and pharmaceutical samples. The use of MWCNTs-COOH vis-à-vis MWCNTs (pure) on the surface of pencil graphite fiber was found advantageous in terms of homogenous and stable coating with enhanced adsorption capacity. The proposed hyphenation approach is recommended to monitor L-met depletion in blood plasma sample as low as 0.016 ng mL^{-1} (and even lower to 0.0099 ng mL^{-1}, LOD, in the present instance) manifesting 677 C→T mutation of MTHFR gene responsible for inborn errors in human beings. The practical utility of the MIMSPE/EC-MIP technique may also be extended to unravel L-met deficiency manifesting several

chronic diseases, viz., AIDS, HIV infection, toxemia, muscle paralysis, depression, and cancer.

Acknowledgements

Authors thank University Grant Commission (UGC), New Delhi for granting research fellowship to A.S. and CSIR for a senior research fellowship to M.P.T. Instrumental facilities were procured out of a recent project (SR/S1/IC-30/2010) funded by the Department of Science and Technology, New Delhi.

Appendix A. Supplementary data

Supplementary data associated with this article can be found, in the online version, at http://dx.doi.org/10.1016/j.jchromb.2012.10.010.

References

[1] B. Gao, Y. Chen, J. Men, J. Chromatogr. A 1218 (2011) 5441.
[2] T.J. Ward, K.D. Ward, Anal. Chem. 82 (2010) 4712.
[3] I. Ciucanu, K.C. Swallow, R. Căpriţă, Anal. Chim. Acta 519 (2004) 93.
[4] B.B. Prasad, M.P. Tiwari, R. Madhuri, P.S. Sharma, Anal. Chim. Acta 662 (2010) 14.
[5] B.B. Prasad, M.P. Tiwari, R. Madhuri, P.S. Sharma, J. Chromatogr. A 1217 (2010) 4255.
[6] B.B. Prasad, M.P. Tiwari, R. Madhuri, P.S. Sharma, J. Chromatogr. B 879 (2011) 364.
[7] Q. Feng, L. Zhao, J.-M. Lin, Anal. Chim. Acta 650 (2009) 70.
[8] A. Mohammadi, Y. Yamini, N. Alizadeh, J. Chromatogr. A 1063 (2005) 1.
[9] C. Malitesta, E. Mazzotta, R.A. Picca, A. Poma, I. Chianella, S.A. Piletsky, Anal. Bioanal. Chem. 402 (2012) 1827.
[10] J.C.C. Yu, E.P.C. Lai, React. Funct. Polym. 66 (2006) 702.
[11] R. Van Brummelen, D. duToit, Amino Acids 33 (2007) 157.
[12] T. Hoshi, S.H. Heinemann, J. Physiol. 531 (2001) 1.
[13] A. Di Rocco, M. Tagliati, F. Danisi, D. Dorfman, J. Moise, D.M. Simpson, Neurology 51 (1998) 266.
[14] S. Toyokuni, K. Okamoto, J. Yodoi, H. Hiai, FEBS Lett. 358 (1995) 1.
[15] V. Lishko, Y. Tan, Methods for treating and reducing the potential for cardiovascular disease using methioninase compositions, US Patent 5,715,835 and PCT/US93/11311 (November 19, 1993).
[16] S. Melnyk, M. Pogribna, I. Pogribny, R.J. Hine, S.J. James, J. Nutr. Biochem. 10 (1999) 490.
[17] X. Sun, Y. Tan, Z. Yang, S. Li, R.M. Hoffman, Anticancer Res. 24 (2005) 59.
[18] K. Iriyama, M. Yoshiura, T. Iwamoto, J. Liq. Chromatogr. 9 (1986) 2955.
[19] L. Dou, I.S. Krull, Anal. Chem. 62 (1990) 2599.
[20] Y.V. Tcherkas, L.A. Kartsova, I.N. Krasnova, J. Chromatogr. A 913 (2001) 303.
[21] R. Vespalec, H. Corstjens, H.A.H. Billie, J. Frank, K.C.A.M. Luyben, Anal. Chem. 67 (1995) 3223.
[22] M.C. Icardo, O.A. Estrela, M. Sajewicz, J.V.G. Mateo, J.M. Calatayud, Anal. Chim. Acta 438 (2001) 281.
[23] M.G. Mingot, J. Iniesta, V. Montiel, R.O. Kadara, C.E. Banks, Sens. Actuators B 155 (2011) 831.
[24] L. Agüí, J. Manso, P.Y. Sedeño, J.M. Pingarrón, Talanta 64 (2004) 1041.
[25] H. Xu, W. Zhang, W. Zhu, D. Wang, J. Ye, K. Yamamoto, L. Jin, Anal. Chim. Acta 545 (2005) 182.
[26] B.B. Prasad, R. Madhuri, M.P. Tiwari, P.S. Sharma, Electrochim. Acta 55 (2010) 9146.
[27] D.A. Skoog, F.T. Holler, T.A. Neiman, Principles of Instrumental Analysis, 5th ed., Harcort Brace College Publishers, Orlando, 1998, p. 13.
[28] A.C. Meng, J. LeJeune, D.A. Spivak, J. Mol. Recognit. 22 (2009) 121.
[29] L. Chen, W. Chen, C. Ma, D. Du, X. Chen, Talanta 84 (2011) 104.
[30] Y. Jinghua, W. Fuwei, Z. Congcong, Y. Mei, Z. Xiaona, W. Shaowei, Biosens. Bioelectron. 26 (2010) 632.
[31] R. Mashima, T.N. Ueda, Y. Yamamoto, Anal. Biochem. 313 (2003) 28.